

文章编号: 2095-4980(2017)04-0646-06

# Permittivity of composites used for Luneburg lens antennas by drilling holes based on 3-D printing technique

DONG Changsheng<sup>1</sup>, CUI Ziqing<sup>1</sup>, LI Yong<sup>1</sup>, WANG Haidong<sup>1</sup>, JIN Chao<sup>1</sup>, YANG Shiwen<sup>2</sup>

(1. Institute of NO. 54, China Electronics Technology Group Corporation, Shijiazhuang Hebei 050081, China;

2. School of Electronic Engineering, University of Electronic Science and Technology of China, Chengdu Sichuan 611731, China)

**Abstract:** Due to the attractive performances such as the ability of beam focus, broadband, multi-beam scanning and other features, Luneburg lens antennas are applied in multi-beam antenna, which overcomes the problem of gain loss produced by multi-beam parabolic antenna. Based on 3-D printing technique, Luneburg lens antennas by drilling holes are studied. Permittivity and loss tangent of the equivalent lens materials can be influenced by original materials, hole shapes, hole directions, and porosity. After tests, polystyrene with waxes may be the most appropriate materials for Luneburg lens with high strength. Permittivity with the shape of triangle is the lowest due to the homogeneity. Relative permittivities with the direction at a range of 15°–45° are lower while loss tangent at a range of 0°–30°. Radial directional holes are more appropriate for Luneburg lens. The relative permittivity is decreased with the increment of porosity. After calculations, the forecasts calculated by Looyenga and A–BG theory are more precise. Finally, Luneburg lens with two layers is fabricated by 3-D printing.

**Keywords:** Luneburg lens by drilling holes; 3-D printing technique; permittivity

**CLC number:** TN804

**Document code:** A

**doi:** 10.11805/TKYDA201704.0646

## 1 Introduction

With the development of satellite communication, radar navigation, aerospace communication, telemetry and remote sensing, all kinds of antennas have wide applications. Luneburg lens possesses a spatially variable refractive index profile, which has been extensively investigated in the past few decades due to its broadband behavior, high gain and the ability to form multiple beams<sup>[1–5]</sup>. It is an attractive gradient index device that can be described by the equation  $n(r) = (2 - r^2/R^2)^{1/2}$ , where  $r$  is the distance from the point inside the lens to the center of the lens, and  $R$  is the radius of the sphere (shown in Fig.1). It has a superior performance compared with conventional uniform material lens that every point on the surface of an ideal Luneburg lens is the focal point of a plane wave incident from the opposite side (the optical path of waves coming into the lens is shown in Fig.1). This special property allows precise direction finding based on amplitude only information as proposed.

Luneburg lens is manufactured as a finite number of concentric homogeneous dielectric shells, which is called a discrete<sup>[6]</sup>. This technique employs different dielectric materials whose relative permittivity covers the range from 1 to 2 and whose loss tangent<sup>[7]</sup> is less than  $10^{-3}$ . However, permittivities of natural dielectric materials are beyond the requirement. Idea dielectric composites can be obtained by the mixture of natural dielectric materials and air (Relative permittivity of air is 1, and loss tangent is nearly 0). There are two kinds of methods to fabricate idea dielectric composites used for Luneburg lens<sup>[8]</sup>: foaming technique and drilling holes technique. Foaming technology is the method that the amount and density of pores in the intershell of materials (such as polystyrene) with low dielectric loss can be controlled by foaming agent<sup>[9]</sup>. Japan obtained various layers with different dielectric constants by this technique in 2005. After assembling these layers along the radius direction, Luneburg lens is achieved<sup>[10]</sup>. Yet it is difficult to adjust the uniformity of pores, which cannot match the requirement of the gradient index inner structure. Drilling holes technique is the method that the amount and density of pores in the intershell are obtained by drilling holes using mechanics<sup>[11]</sup>. Zimmerman proposed a method to eliminate the needs for dielectrics with different curvatures and different permittivities

**Received date:** 2015-11-16; **Revised date:** 2016-03-09

**Foundation item:** This work was supported by the Science and Technology Programme of Shijiazhuang under Grant 151130081A.

by drilling radial holes in a homogeneous dielectric sphere. The radius change with position in the sphere in order to produce an approximation of the continuous Luneburg distribution<sup>[12]</sup>. Rondineau separates the sphere into slices. The holes are drilled in per slice. This technique provides a much easier and cheaper process<sup>[11]</sup>. Strickland separates the sphere into wedge with the same angle. Holes with various diameters and densities are drilled upright to the wedge to change the permittivities<sup>[13]</sup>. However, the orientation and accuracy are difficult to improve because of distortion and low mechanical intensity. Moreover, the inaccuracies in the curved shell manufacturing process produce intershell air gaps, which degrade the performance of the lens. It is demonstrated that the efficiency will degrade to 21.5% in the Ka band when the intershell air gaps reach to 0.1 times of the wavelengths<sup>[18]</sup>. So the conventional methods of fabricating spherical Luneburg lens are great challenges and the spherically focal surface, which is incompatible with the planar feed source or detector array, also prevents its development and further applications. Besides, the conventional methods are quite expensive and time consuming.

To avoid these disadvantages, this paper proposes that Luneburg lens is fabricated by 3-D printing technique. 3-D printing is a rapid prototyping process, which is one of such technique that employs ink-jet printing technology for processing powder. A thin layer of powder is deposited in a workspace container and the powder is then fused together using laser beam that traces the shape of the desired cross section. The process is repeated by depositing layers of powder thus building the part layer by layer. Powder is selectively consolidated into a part and the remaining powder can be removed. By using this technique, no support structures, mould and tools are typically required to create complex shapes. Luneburg lens can be fabricated without intershell air gaps and the number, density and accuracy of pores can be guaranteed by the computers, which can promise that dielectric properties are close to the design. However, influence of dielectric properties of Luneburg lens produced by 3-D printing is vague. And other details about this technique are also discussed in this paper.

## 2 Experiment details

### 2.1 Permittivity

Permittivity can be described as followed,

$$\varepsilon^* = \varepsilon_r(1 - j \tan \delta) \quad (1)$$

$\varepsilon_r$  and  $\tan \delta$  are relative permittivity and loss tangent, respectively. Permittivity is vital to the performance of Luneburg, which requires that permittivity reduce from inner to outer along the radius. Permittivity of materials produced by laser sintering is different to the common. So the original data must be tested. The theory of test can be shown as Fig.2. Test accuracy of this system can be 0.001 by the calculation and test.

Cylindrical cavity is fabricated with the diameter of 60.2 mm and length of 58.5, which is adopted to transmit the electromagnetic wave. The sample is inserted into the bottom of cylindrical cavity. Intrinsic frequency of cylindrical cavity changes after inserting the sample. Permittivity of the materials can be calculated by the change of intrinsic frequency<sup>[14]</sup>. The  $Q$  of the cavity is 26 358. There are no specific requirements on the samples.

### 2.2 Test Sample

The dimension of sample is the diameter of 60 mm, the thickness of 4.5 mm. Permittivity of samples can be influenced by materials, shapes, directions and porosity. All these are discussed in this paper. Various materials can be used in 3-D printing. Nylon (PA12), Acrylonitrile-Butadiene-Styrene(ABS), Polystyrene (PS), Photosensitive Resin (PR) are tested

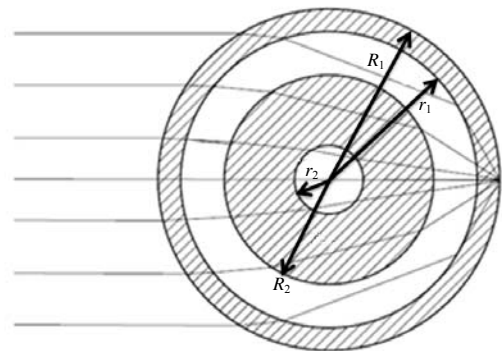


Fig.1 Theory diagram of Luneburg lens' focus

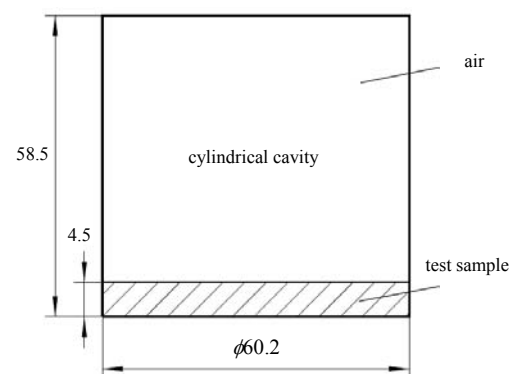


Fig.2 Cylindrical cavity methods

due to the requirement that relative permittivity covers the range from 1 to 2 and loss tangent is less than  $10^{-3}$ . By this test, appropriate materials are chosen. The shapes of drilled holes can only be circle owing to the restriction of the drilling tools. Yet shapes and direction can be easily changed by 3-D printing. However, the influences of the shapes and directions of the holes are obscure. So various shapes are chosen for test, such as circle, triangle, square and hexagon. Besides, various directions are also tested. Porosity is vital to permittivity, which can be adjusted by various ratios of dielectric materials and air. The more the air is, the lower the permittivity is. The influence is discussed.

Based on the discussion, the samples tested are shown in Table1. All these samples are fabricated by EOS equipment (FORMIGA P110) provided by Shanghai Ureal Technology, Co., Ltd.

Table1 Samples fabricated by 3-D printing

No.	materials	shape	direction/(°)	porosity/(%)	test
1	PA12	solid	—	0	materials
2	ABS	solid	—	0	
3	PS	solid	—	0	
4	PS mixed with wax(PSW)	solid	—	0	
5	PS mixed with resin(PSR)	solid	—	0	
6	PR	solid	—	0	
7	PA12	circle	0	55	shape
8	PA12	triangle	0	55	
9	PA12	square	0	55	
10	PA12	hexagon	0	55	direction
11	PA12	hexagon	15	55	
12	PA12	hexagon	30	55	
13	PA12	hexagon	45	55	
14	PA12	hexagon	60	55	
15	PA12	hexagon	0	42.13	porosity
16	PA12	hexagon	0	67.92	
17	PA12	hexagon	0	82.24	

### 3 Results and discussion

Sample 10 fabricated by 3-D printing is shown in Fig.3. Other samples with various materials, shapes, directions and porosity can also be fabricated. The dimensional errors of samples can be controlled below 0.2 mm.

#### 3.1 Materials

The influence of various materials on the permittivity by 3-D printing is shown in Table2.

PR cannot be tested owing to larger permittivity loss by using cylindrical cavity method, which means it cannot be used in Luneburg lens. Except that, other results obtained in test are below the data from handbooks, which had relationships with 3-D printing technique. Minor pores that cannot be found by eyes exist in the samples by 3-D printing. Because the permittivity of air is lower than materials, permittivity of samples with minor pores is lower. It can be influenced by processing parameters of 3-D printing.

Among various materials, the permittivity of PS owns the least value, which means PS is the most appropriate material for Luneburg lens. However, the toughness of PS is lower and PS is easier to crack. In order to prevent the cracks and brittleness, wax and resin are infiltrated into samples. When minor pores are filled with wax or resin, samples are strengthened (PSW and PSR). Relative permittivity of the mixture (PSW) increases by 30%, while loss tangent reduces by 12.5%. But the relative permittivity of the mixture (PSR) increases by 72%, and the loss tangent cannot meet the requirements. So PSR cannot be used for Luneburg lens.

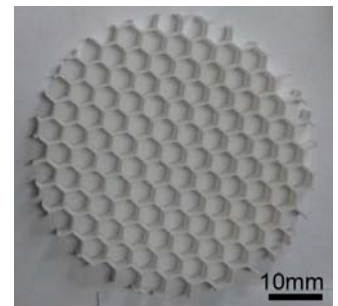


Fig.3 Sample 10 fabricated by 3-D printing

Table2 Permittivities of various materials

materials	relative permittivity(14 GHz)		loss tangent(14 GHz)	
	test	handbook	test	handbook <sup>[15]</sup>
PA12	2.748	4.5	$9.0 \times 10^{-3}$	0.02
ABS	3.489 8	2.4–3.8	$5.5 \times 10^{-3}$	0.009
PS	1.83	2.45–2.65	$1.6 \times 10^{-3}$	0.0001
PSW	2.383	—	$1.4 \times 10^{-3}$	—
PSR	3.152	—	$2.8 \times 10^{-2}$	—
PR	—	—	—	—

### 3.2 Shapes

In order to research the influence of shapes on the permittivity, the following requirements must be obeyed: 1) Area of single pore must be the same; 2) Areas of all pores must be the same. Table 3 lists the results. Various shapes can change the permittivity slightly. Permittivity with the shape of triangle is the smallest due to the homogeneity.

### 3.3 Direction

The influences of direction of holes on the permittivity are shown in Fig. 4. Relative permittivities are lower at a range of  $15^\circ$ – $45^\circ$  while loss tangent at a range of  $0^\circ$ – $30^\circ$ . There are two ways of drilling holes: vertical direction and radial direction. Different incidence directions present various angles in Luneburg lens with vertical direction holes. It will deteriorate the permittivity, which will cause low efficiency and directional pattern. Rondineau pointed out that the efficiency decrease from 30% at 26.5 GHz down to 15% at 32 GHz in Luneburg lens with vertical direction holes. It can be concluded that radial directional holes are more appropriate for Luneburg lens<sup>[11]</sup>.

### 3.4 Porosity

The influence of porosity on the permittivity is shown in Fig. 5. Permittivities will cause a dramatic decrease due to reduction of the thickness and volume when the porosity increases. Relative permittivity (2.748) and loss tangent ( $9 \times 10^{-3}$ ) of PA12 are all larger than that of the air (relative permittivity is 1 while loss tangent is 0). The composite consists of dielectric materials and air. The ratio of dielectric materials and air, which can be regarded as porosity, can strongly influence permittivities. The more volume of air is, the lower the permittivity is.

Relative permittivity of the composite can be calculated by effective media theory. At present, there are many effective media theories as followed:

$$\text{CM(MG): } \frac{\varepsilon_{\text{eff}} - \varepsilon_h}{\varepsilon_{\text{eff}} + 2\varepsilon_h} = p \frac{\varepsilon_l - \varepsilon_h}{\varepsilon_l + 2\varepsilon_h} \quad (2)$$

$$\text{A-BG: } \frac{\varepsilon_l - \varepsilon_{\text{eff}}}{\varepsilon_l - \varepsilon_h} = (1-p) \left( \frac{\varepsilon_{\text{eff}}}{\varepsilon_h} \right)^{\frac{1}{2}} \quad (3)$$

$$\text{Looyenga: } \varepsilon_{\text{eff}} = \left[ (\varepsilon_l^{\frac{1}{3}} - \varepsilon_h^{\frac{1}{3}})p + \varepsilon_h^{\frac{1}{3}} \right]^3 \quad (4)$$

$$\text{Maxwell: } \varepsilon_{\text{eff}} = \varepsilon_h + 3p \frac{\varepsilon_l - \varepsilon_h}{\varepsilon_l + 2\varepsilon_h} \varepsilon_h \quad (5)$$

Where  $\varepsilon_{\text{eff}}$  is effective relative permittivity of composite;  $\varepsilon_l$  is relative permittivity of dielectric materials (PA12: 2.748);  $\varepsilon_h$  is relative permittivity of air (air: 1);  $p$  is the porosity. Effective relative permittivity is calculated in Fig. 6. The calculations with Looyenga theory and A-BG theory show minor error, which is closer to the experimental result. Moreover, errors between calculations and experimental results decrease with the increment of porosities. It can be inferred that the calculation at outer layers of Luneburg lens can be more accurate than inner layers.

Besides, the unit loss of materials can be expressed as followed,

$$w = \text{Re} \left[ \frac{1}{2} E \cdot J^* \right] = \text{Re} \left[ -\frac{1}{2} j \omega \varepsilon^* E^* \cdot E \right] = \text{Re} \left[ -\frac{1}{2} j \omega \varepsilon_{\text{eff}} (1 - j \tan \delta) E^2 \right] \quad (6)$$

Where  $E$  is electrical field value and  $J$  is the energy. It is obvious that the unit loss of materials has relationships with effective relative permittivity, which can also be influenced by the porosity. The trends of experimental results (relative permittivity and loss tangent) are equal to the theory.

Table 3 Dielectric properties of the holes with various shapes

shape	relative permittivity(14 GHz)	loss tangent(14 GHz)
circle	1.547	$5.0 \times 10^{-3}$
triangle	1.522	$4.0 \times 10^{-3}$
square	1.546	$4.1 \times 10^{-3}$
hexagon	1.574	$4.3 \times 10^{-3}$

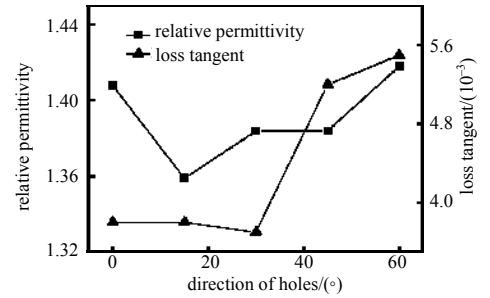


Fig. 4 Influence of angle on the permittivity

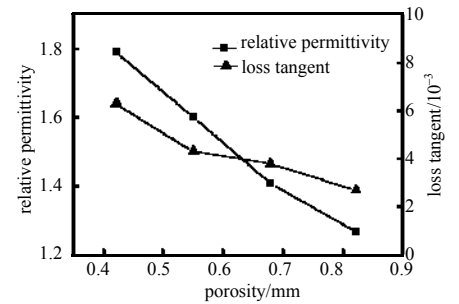


Fig. 5 Influence of porosity on the permittivity

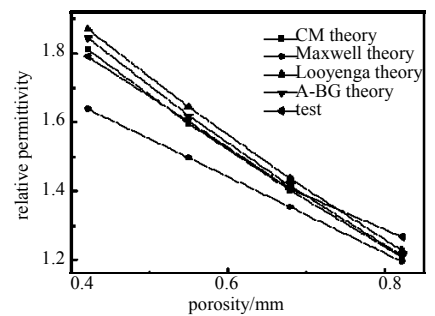


Fig. 6 Comparison of calculation and test

### 3.5 Luneburg lens

The Luneburg lens is optimized by differential evolution algorithm. The optimization results show that Luneburg lens can achieve optimal gain. By using optimization algorithms to optimize the lens antenna, a two-layered Luneburg lens antenna with an optimized gain performance is designed.

After the investigation and design, appropriate parameters for 3-D printing are chosen. Luneburg lens with two layers is fabricated shown in the Fig.7. Vertical direction holes are applied in the inner layer to wipe off the powders unsintered, while radial direction holes are applied in the outer layer to improve the efficiency and directional patterns. Detailed parameters are shown in Table 4. Holes on the layers tapered from outer to inner, which are of the shape of coniform.

The performance of Luneburg lens fabricated by 3-D printing is tested. Fig.8 gives the gain of Luneburg lens fabricated by 3-D printing with a value of 19 dB to 22.5 dB across 12.0 GHz to 15.0 GHz, which can satisfy the design requirements.

## 4 Conclusion

3-D printing technique is applied to fabricate Luneburg lens. Fundamental parameters are investigated in this paper. It can be concluded that the permittivity of PS is the least. PSW may be the most appropriate material for Luneburg lens with high strength. However, relative permittivity of PSW increase by 30% and loss tangent decreases by 12.5%. Permittivity with the shape of triangle is the lowest due to the homogeneity. Relative permittivities with the direction at a range of  $15^{\circ}$ – $45^{\circ}$  are lower while loss tangent at a range of  $0^{\circ}$ – $30^{\circ}$ . Radial directional holes are more appropriate for Luneburg lens. The relative permittivity decreases with the increase of porosity. After calculations, the forecasts calculated by Looyenga and A-BG theory are more precise. Finally, Luneburg lens with two layers is fabricated by 3-D printing technique, which is closer to the design result.

### Reference:

- [1] MITCELL-THOMAS R C, QUEVEDO-TERUEL O, MCMANUS T M, et al. Lenses on curved surfaces[J]. Optics Letters, 2014, 39(12):3551–3554.
- [2] LIU J. Research on multi-beam Luneburg lens antenna[D]. Chengdu, China: University of Electronic Science and Technology of China, 2010.
- [3] LIU F, ZHU Z B, CUI W Z, et al. Application of terahertz techniques in space science[J]. Journal of Terahertz Science and Electronic Information Technology, 2013, 11(6):857–866.
- [4] NIKKHAH H, HALL T. Metamaterial Luneburg lens for Fourier optics on a chip[C]// Proc. SPIE 8988. San Francisco, California, United States: SPIE, 2014.
- [5] DHOUOUBI A, BUROKUR S N, DE L A. Planar metamaterial-based beam-scanning broadband microwave antenna[J]. Journal of Applied Physics, 2014, 115(19):194901.
- [6] PFEIFFER C, GRBIC A. A printed broadband Luneburg lens antenna[J]. IEEE Transactions on Antennas and Propagation, 2010, 58(9):3055–3059.
- [7] MATEO S C, DYKE A, HAQ S, et al. Flat Luneburg lens via transformation optics for directive antenna applications[J]. IEEE Transactions on Antennas and Propagation, 2014, 62(4):1945–1953.
- [8] WU X, LAURIN J J. Fan-beam millimeter-wave antenna design based on the cylindrical Luneberg lens[J]. IEEE Transactions on Antennas and Propagation, 2007, 55(8):2147–2156.

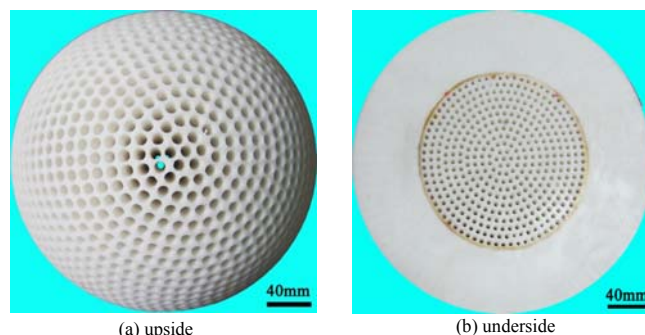


Fig.7 Luneburg lens fabricated by 3-D printing

Table 4 Parameters of Luneburg lens with two layers

	radius/mm	number of holes	porosity/%	relative permittivity
inner layer	61.29	416	26.42	1.950 18
outer layer	111.59	1 177	29.31	1.905 95

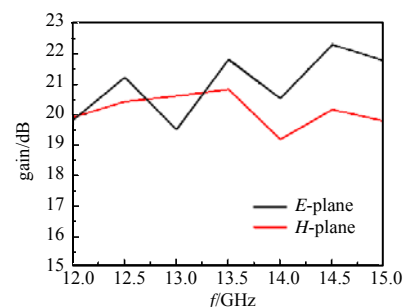
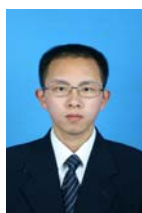


Fig.8 Gain of Luneburg lens fabricated by 3-D printing

- [9] BOR J, LAFOND O, MERLET H, et al. Technological process to control the foam dielectric constant application to microwave components and antennas[J]. IEEE Transactions on Components, Packaging and Manufacturing Technology, 2014, 4(5): 938–942.
- [10] Japanese style society. Fabrication methods of Luneburg lens[P]. CN101057370, 2005.
- [11] RONDINEAU S, HIMDI M, SORIEUX J. A sliced spherical Luneburg lens[J]. IEEE Antennas and Wireless Propagation Letters, 2003, 2(1): 163–166.
- [12] ZIMMERMAN A J. Luneburg lens and Methods of Constructing Same[P]. U.S. Patent 5–677–796, 1995.
- [13] STRICKLAND Peter C. Method fabricating Luneburg lenses[P]. US6721103B1, 2004.
- [14] ZHONG M H. Research on Luneburg lens antenna with stratified drilled holes structure[D]. Chengdu, China: University of Electronic Science and Technology of China, 2009.
- [15] WANG W G, TIAN Y C, LV T J. Choose of Plastics[M]. Beijing: Chemistry Industry Press, 2007.

#### About the author:



**DONG Changsheng**(1984–), was born in Shijiazhuang, Hebei province. Senior Engineer. Current research involves functional composites used in the antenna. email: dongcs07@gmail.com.

**CUI Ziqing**(1988–), was born in Shijiazhuang, Hebei province. Engineer. Current research involves antenna design.

**LI Yong**(1978–), was born in Shijiazhuang, Hebei province. Professor. Current research involves antenna and terahertz technology.

**WANG Haidong**(1980–), was born in Chengde, Hebei province. Senior Engineer. Current research involves composites and forming technology.

**JIN Chao**(1964–), was born in Xinyang, Henan province. Professor. Current research involves antenna forming technology.

**YANG Shiwen**(1967–), was born in Shijiazhuang, Hebei province. Senior Engineer. Current research involves antenna theory and technology.